AJP

ISSN : 0971 - 3093

Vol 28, Nos 10-12, October-December 2019

ASIAN JOURNAL OF PHYSICS

An International Peer Reviewed Research Journal

Advisory Editors : W. Kiefer & FTS Yu

A Special Issue

Dedicated to

Prof Kehar Singh

Formerly Professor of Physics

at IIT Delhi

Guest Editor : R. S. Sirohi

ap

ANITA PUBLICATIONS

FF-43, 1st Floor, Mangal Bazar, Laxmi Nagar, Delhi-110 092, India

B O : 2, Pasha Court, Williamsville, New York-14221-1776, USA

Asian Journal of Physics

(A Non-Profitable Publication)

ap

Asian Journal of Physics
Vol. 28, Nos 10-12 (2019) 1149-1160
Available on: www.asianjournalofphysics.in

Investigations of magnetic resonances with modulated laser excitation in the atomic medium for magnetometry applications

Gour S Pati and Renu Tripathi*
Division of Physics, Engineering Mathematics & Computer Science (PEMaCS),
Delaware State University, Dover, DE 19901, USA

This article is dedicated to Prof Kehar Singh for his significant contributions to Optics and Photonics

We have investigated magnetic resonances produced by resonant laser excitation of the atomic medium with modulated light. Magnetic resonances in two different atomic media are studied. First, we have studied magnetic resonances using laser excitation of D_1 transition in a pure isotope rubidium cell. We explain the origin of magnetic resonances using two-photon Lambda transitions, and simulate magnetic resonances using a theoretical model based on the density-matrix equations. Second, we have studied magnetic resonances in fluorescence from a sodium cell. This study is intended for performing remote magnetometry experiments with mesospheric sodium atoms. We have also demonstrated a new correlation technique, which can be performed over a wide frequency range for measuring an unknown magnetic field in magnetometry. Present studies are aimed towards improving our understanding of magnetic resonances for magnetometry applications.

Keywords: Nonlinear magneto-optic rotation (NMOR), Alkali Atoms, Magnetometry

1 Introduction

This article is affectionately dedicated to Professor Kehar Singh, our graduate (Ph D and M Tech) thesis advisor, at the Indian Institute of Technology Delhi (IITD). Both authors, Tripathi and Pati have had the privilege of working and associating with Professor Singh for more than 25 years. He has been a wonderful mentor, teacher and an overall a great role model for us. We have learnt to persevere, and work sincerely from him. It still amazes and inspires us to see and follow his dedication to Optics and Photonics.

Measuring magnetic field with high precision and high spatial resolution has many potential applications [1]. For instance, detection of weak magnetic field distribution can provide a new noninvasive diagnostic method for heart and brain activities [2]. It is also key to magnetic anomaly detection used in a wide range of military applications [3]. Atomic magnetometers (AMs) are the systems of choice in these applications since they can achieve high sensitivity via resonant light-atom interaction. AMs have been used in practical applications in space physics, geomagnetism, medical imaging and ocean science [1]. They can be miniaturized to design low-cost sensor arrays for conducting magnetic surveillance in automated platforms [4,5]. Over the years, a wide range of techniques has been developed in atomic magnetometry to measure the response of atomic angular momentum to the external magnetic field [1,6,7]. Most atomic magnetometers use quantum interference effect produced by optical pumping. Optical pumping in alkali atoms (e.g. Rb, Cs, Na and K) creates spin alignment, and the response of spin to the external magnetic B field is determined by measuring the precession (or Larmor) frequency ($\Omega_L = \beta\gamma$, γ is the gyromagnetic ratio of atom) through the magnetic resonance produced by resonant (or near-resonant) excitation with light.

Corresponding author :
e-mail:rtripathi@desu.edu (Renu Tripathi)

The sensitivity of the atomic magnetometer is decided by the linewidth of magnetic resonance, and the noise sources present in the system. Magnetic resonance using nonlinear magneto-optical rotation (NMOR) can produce high sensitivity in atomic magnetometer due to cancellation of common-mode noise [8]. Resonant excitation with modulated light can produce build-up of atomic polarization by synchronous optical pumping, and magnetic resonance for non-zero field. This increases the dynamic range of atomic magnetometer in magnetic field measurement. The modulation strategy can also be used to measure high B field in the geophysical range [9-11]. In this paper, we investigate the physical origin of magnetic resonances produced by laser excitation of the atomic medium with amplitude modulated light. We describe the interaction between multilevel atom and coherent laser field in terms of quantum interference between the ground-state magnetic sublevels. We discuss results obtained from two different experiments: (a) NMOR resonance obtained using laser excitation of D_1 transition in rubidium vapor, and (b) fluorescence resonance using laser excitation of D_2 transition in sodium vapor. Intensity correlation between two orthogonally polarized laser fields is performed to demonstrate an alternative method for measuring magnetic resonance in the NMOR configuration. High agnetic field resonances are measured in fluorescence from a sodium cell to demonstrate suitability of doing remote magnetometry with mesosphere sodium atoms.

2 Theoretical Discussion

Magnetic resonance can be observed in several different geometries of laser polarization $\vec{E}$ and magnetic field $\vec{B}$ directions. To simplify our discussion, we consider $\vec{B}$ perpendicular to $\vec{E}$, direction of $\vec{B}$ as the axis of quantization, and laser excitation with linearly polarized light with $\vec{E}$ having σ^+ and σ^- components. We use a theoretical model using density-matrix equations to simulate interaction of atoms with light [12]. We consider laser excitation of $F_g = 1 \rightarrow F_e = 0$ transition by linearly polarized light as shown in Fig 1a. In this case, Fig 1b shows a magnetic resonance in absorption (or fluorescence) produced with a dip at $B = 0$. This is known as Hanle resonance [13]. The resonance is formed due coupling of two ground-state magnetic sublevels ($m_F = -1$ and $+1$) by a $\Lambda-$ transition as shown in Fig 1a. The two-photon $\Lambda-$ transition between the two ground-state Zeeman sublevels forms a 'dark state', which leads to minimum absorption at $B = 0$. When $B \neq 0$, two-photon resonance condition is not satisfied, leading to increase in absorption (or fluorescence). Figure 1c shows the magnetic resonance calculated using polarization rotation, also known as NMOR. Unlike the resonance in absorption (Fig 1b), polarization rotation produces a dispersive magnetic resonance with a zero-crossing at $B = 0$. This resonance can also be produced by near-resonant laser excitation associated with reduced absorption. Even though, we have shown the magnetic resonance using a simple atomic model with laser excitation of $F_g = 1 \rightarrow F_e$ leading to increase in absorption (or fluorescence). Figure 1c shows the magnetic resonance calculated using polarization rotation, also known as NMOR. Unlike the resonance in absorption (Fig 1b), polarization rotation produces a dispersive magnetic resonance with a zero-crossing at $B = 0$. This resonance can also be produced by near-resonant laser excitation associated with reduced absorption. Even though, we have shown the magnetic resonance using a simple atomic model with laser excitation of $F_g = 1 \rightarrow F_e = 0$ transition, similar magnetic resonance can be formed by considering laser excitation of $F_g = 1 \rightarrow F_e = 1$ transition and $F_g = 2 \rightarrow F_e = 2$ transition with linearly polarized light in the atomic model. In case of $F_g = 2 \rightarrow F_e = 2$ transition, multiple $\Lambda-$ systems are formed with $\Delta m_F = 2$ creating multiple 'dark states' not interacting with light. The line width of magnetic resonance corresponds to the inverse of ground-state decoherence time between the magnetic sublevels, which can very long (>100ms) in anti- relaxation (e.g. paraffin) coated cells. This suggests that Hanle resonance at B = 0 can be used to perform near-zero magnetic field measurements with extremely high sensitivity ($<100\, f\, T/\sqrt{Hz}$). However, Hanle resonance gives a very low dynamic range in magnetic field measurement.

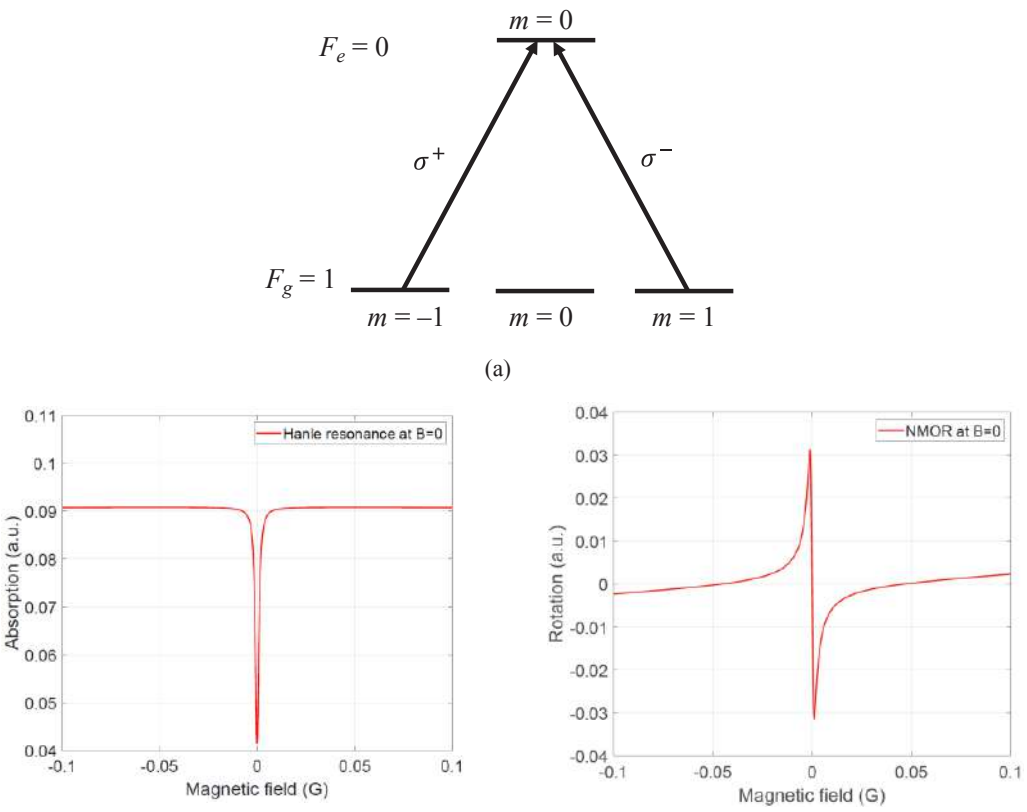

Fig 1. (a) Energy diagram showing a Λ– system formed in laser excitation of $F_g = 1 \rightarrow F_e = 0$ transition by linearly polarized light, and theoretical calculations showing magnetic resonance produced by this Λ– system in (b) absorption and (c) polarization rotation.

Magnetic resonances with dips at $B \neq 0$ are formed only if the laser beam is modulated at the Larmor frequency Ω_L. This can be explained by using multiple Λ– systems and 'dark states' formed by multiple frequency components of the modulated laser beam with modulation frequency Ω_m. The modulated laser beam has frequency sidebands which are offset by $\pm n\,\Omega_m$, $n = 1, 2, \ldots$ from the carrier (or laser) frequency ω_0. Figure 2a shows a Λ–system formed in laser excitation of $F_g = 1 \rightarrow F_e = 0$ transition by the carrier ω_0 and the side band $\omega_0 - \omega_m$. In this case, the center of magnetic resonance satisfies the two-photon resonance condition $\Omega_m = 2\,\Omega_L$. Magnetic field can be measured by finding the center(i.e. dip) of magnetic resonance at $B = \Omega_m/2\gamma$. Higher-order frequency sidebands of modulated beam can also form other Λ– systems giving rise to higher-ordermagnetic resonances. Figure 2b shows magnetic resonances produced in polarization rotation,calculated using our theoretical model simulating laser excitation of $F_g = 2 \rightarrow F_e = 1$ transition in rubidium (^{87}Rb) atom with modulated light (Ω_m = 50 kHz). The magnetic field $\vec{B}$ used in our simulation is parallel to the direction of light propagation. In this case, zero-field Hanle resonance is produced at $\Omega_L = 0$ higher-order magnetic resonances with centers matching resonance condition $\Omega_L = \pm\,\Omega_m/2$ are also produced by modulated laser excitation. Calculated resonances in Fig 2c have dispersive line shapes, and are known as NMOR resonances. The physical origin of higher order resonances formed at $\Omega_L = \pm\,\Omega_m/2$ is already explained by choosing direction of $\vec{B}$ as the axis of quantization. Linearly polarized light with $\vec{E}$ in this axis of quantization can be assumed to form Λ– systems involving both σ^+ and σ^- excitations as shown in Fig 2b.

The two-photon resonance condition for such a Λ– system will correspond to $\Omega_L = \pm \Omega_m/2$ (or $B = \pm \Omega_m/2\gamma = \pm 35.7$ mG) for $\gamma \simeq 0.7$ MHz/G as shown in Fig 2c. Weak resonances at $\Omega_L = \pm \Omega_m$ are also produced by Λ– systems formed by the frequency sidebands $\omega_0 \pm \Omega_m$ of modulated light. Next, we report experimental observation of these magnetic resonances in atomic vapor cells using modulated laser excitation.

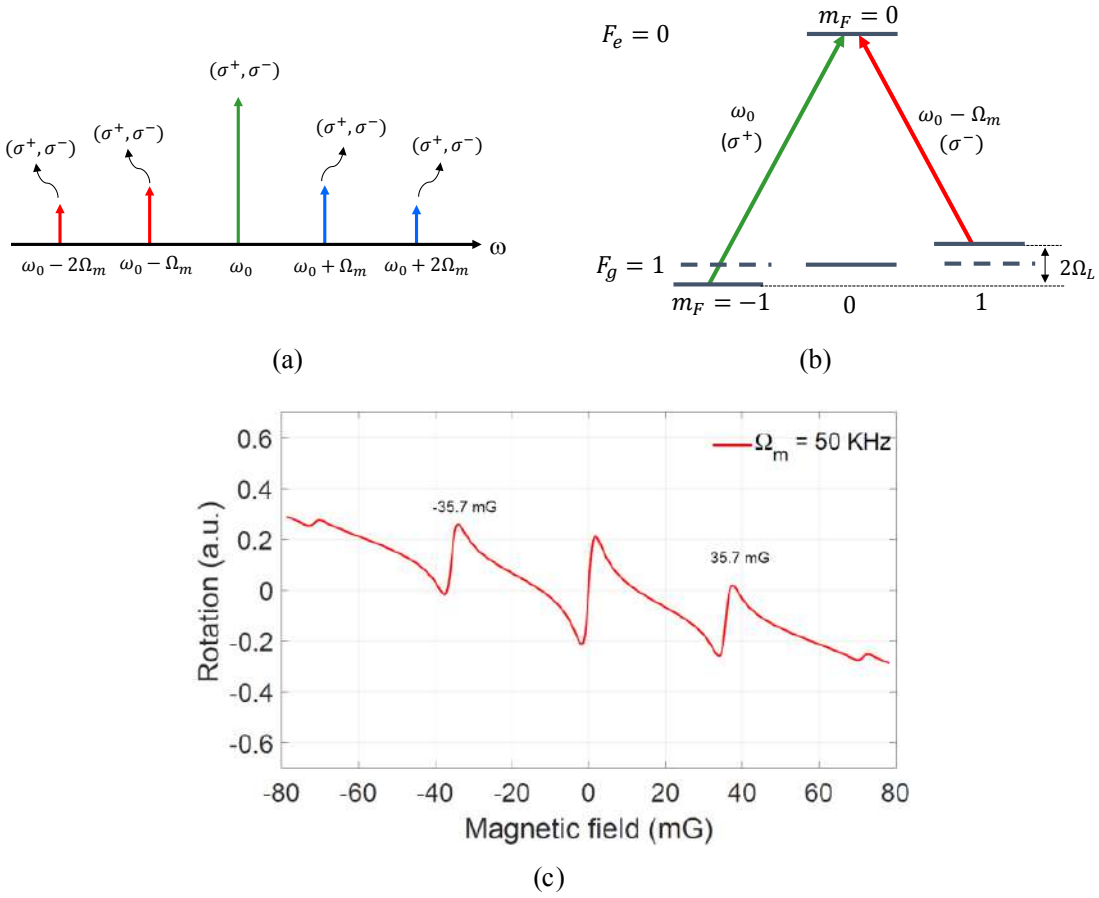

Fig 2. (a) Frequency spectrum of modulated light, (b) Λ– system formed by carrier ω_0 and sideband $\omega_0 - \Omega_m$ in $F_g = 1 \rightarrow F_e = 0$ transition by σ^+ and σ^- components of linearly polarized light and (c) theoretical calculation showing magnetic resonance in polarization rotation produced by laser excitation of $F_g = 2 \rightarrow F_e = 1$ transition in a ^{87}Rb atom with modulated light.

3 Experimental Description

The schematic diagram of the experimental setup is shown in Fig 3. A narrow-band diode laser tuned to resonance with rubidium D_1 transition ($\lambda \simeq 795$ nm) is used in the experiment. Part of the laser beam is sent through a reference rubidium cell to lock the laser frequency to a particular atomic transition using a laser servo. The remaining laser beam is modulated using an acoustic-optic modulator (AOM). The first-order diffracted beam from the AOM is used as a probe beam in the experiment. Using a half wave plate (HWP), the light polarization is set to a particular linear polarization state. We used a pure-isotope ^{87}Rb vapor cell (optical length = 2.3 cm, diameter = 1 cm) filled with 10 Torr neon buffer gas. The cell is placed at the center of a custom-made mu-metal magnetic shield enclosure, which attenuates the ambient magnetic

field by approximately 30 dB.Axial magnetic field along the direction of light propagation is applied using a pair of Helmholtz coils placed inside the enclosure. The magnetic field is scanned using a low-noise current source. The cell is wrapped with bifilar twisted (to cancel the residual magnetic field produced due to heating) and polymide insulated nichrome heating wire, and is heated to a steady temperature of 53 °C to produce rubidium vapor with high density (10^{11} – 10^{12} atoms/cm^3).

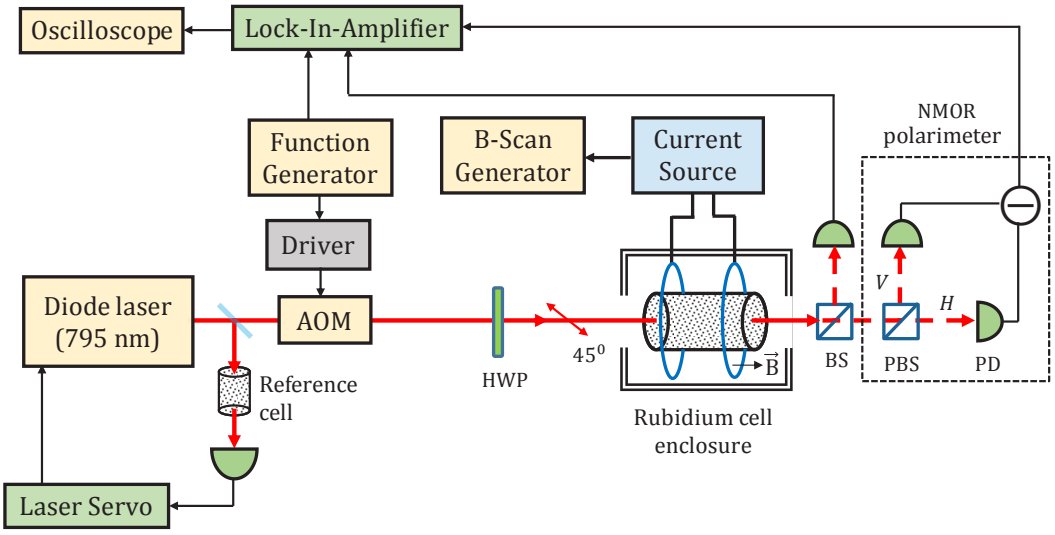

Fig 3. (a) Schematic diagram of the experimental setup used to measure magnetic resonances with modulated laser excitation in a rubidium cell. Magnetic field is directed along the light propagation direction, and 45° linearly polarized light is utilized to measure the NMOR resonances in polarization rotation.

We used a polarimeter to measure polarization rotation and observe NMOR magnetic resonance in transmitted light. Polarization rotation is measured by sending light through a polarizing beam splitter (PBS) and subtracting resulting light intensities in horizontal (H) and vertical (V) polarization channels with an electronic subtractor. Magnetic resonances are observed by demodulating the subtracted signal from the polarimeter with a lock-in-amplifier. We have also done experiments with a sodium cell to observe magnetic resonance in fluorescence. The experimental setup for sodium cell is similar to that shown in Fig 3. In this case, a narrow-band frequency-doubled Raman fiber amplifier laser is used and the laser is tuned to sodium D_2 line ($\lambda = 589.15$ nm). A reference sodium cell is used in the laser servo setup to lock the laser to different sodium D_2 transitions. The experimental sodium cell was placed inside a two-layered magnetic shield enclosure. Three-axis Helmholtz coils were installed inside the shield to further reduce ambient field by canceling the residual magnetic field with coils. Coils along the vertical y-axis (or horizontal x-axis) perpendicular to the light propagation direction are utilized to apply fixed or scanning magnetic field, as per our experimental needs. In this case, instead of using linear polarization, light polarization is set to circular using a quarter-wave plate (QWP) (not shown in Fig 3). Temperature of the Na cell was kept at 86°C. Magnetic resonances produced in fluorescence from sodium cell at 90° angle to the light propagation direction are measured.

4 Results and Discussion

First, we discuss our results obtained from the rubidium cell experiment. Figure 4a shows zero-field Hanle resonances produced by scanning the magnetic field along the laser beam propagation direction, and tuning the laser to produce continuous excitation of $F_g = 2 \rightarrow F_e = 1$ transition in ^{87}Rb atoms in the cell. Light

is linearly polarized at 45° angle using a HWP. The resonances are measured in transmitted light through the cell. Figure 4a shows the effect of power broadening on Hanle resonance by increasing the optical power in laser excitation from 20 to 200 μW. The origin of zero-field Hanle resonance is already explained using 'dark states' formed by two-photon Λ– transitions between the ground-state magnetic sublevels. We measured the linewidth of Hanle resonance for 20 μW by fitting the resonance profile with a Lorentzian function, and found FWHM = 1.16 mG (or 0.81KHz). The linewidth of resonance for 200 μW is 3.12 mG (or 2.19 KHz). The broadening of resonance linewidth is caused due to increase in optical power in laser excitation by ten fold. The fundamental linewidth of Hanle resonance is decided by the medium decoherence time. We also measured the zero-field magnetic resonance in polarization rotation (or NMOR) using the polarimeter configuration shown in Fig 3. In this case, resonance has a dispersive line shape. Figures 4(b,c) show a comparison of zero-field NMOR resonances by tuning laser excitation from $F_g = 2 \rightarrow F_e = 1$ to $F_g = 1 \rightarrow F_e = 2$ transition in ^{87}Rb atoms. The NMOR resonance changed sign (i.e. from down-up to up-down) when the laser is tuned to $F_g = 1 \rightarrow F_e = 2$ transition. This can be explained due to the fact that the excited-state contains more magnetic sublevels than the ground-state for $F_g = 1 \rightarrow F_e = 2$ transition. As a result, in addition to Λ– transitions, V – transitions between excited-state Zeeman sublevels are formed, causing increase in absorption (or sign change in NMOR) at the line center, an effect which is known as electromagnetically induced absorption (EIA) [14].

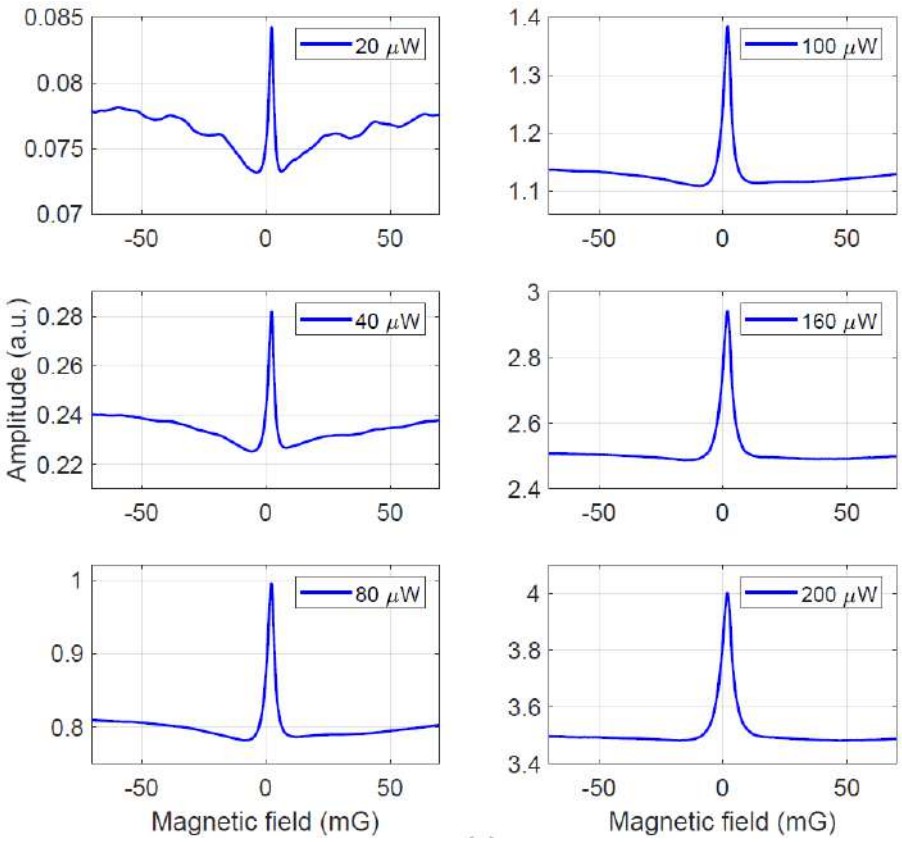

(a)

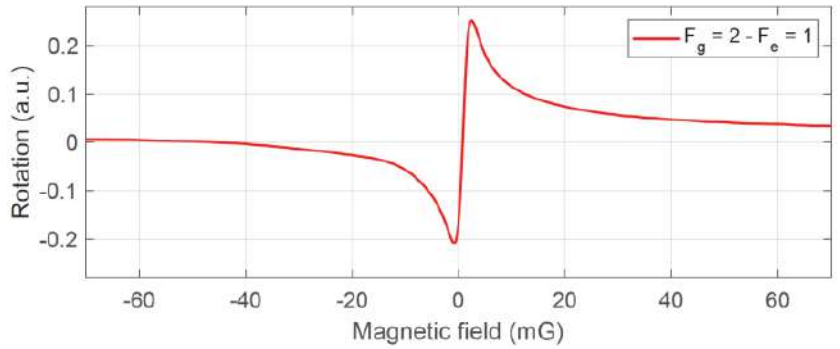

(b)

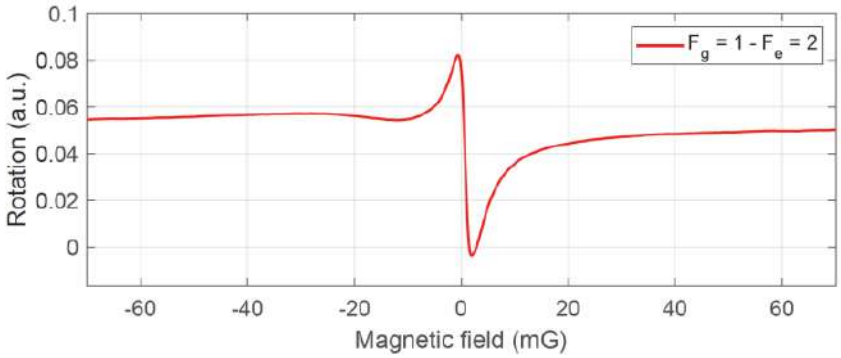

(c)

Fig 4. (a) Zero-field Hanle resonances obtained for different optical power and continuous laser excitation of $F_g = 2 \rightarrow F_e = 1$ transition in ^{87}Rb atoms, (b) & (c) NMOR resonances showing change in sign while tuning the laser from $F_g = 2 \rightarrow F_e = 1$ to $F_g = 1 \rightarrow F_e = 2$ transition in ^{87}Rb atoms.

Next, we discuss magnetic resonances produced by laser excitation of $F_g = 2 \rightarrow F_e = 1$ transition in ^{87}Rb atoms with modulated light. The laser beam is modulated by sending pulses with frequency Ω_m = 50 kHz and duty cycle, DC = 50% to the AOM driver shown in Fig 3. Average power of the laser beam was set to 100 µW. Figure 5a shows the in-phase and quadrature components of NMOR magnetic resonances measured as a function of the axial B field using a two-channel lock-in-amplifier. The in-phase component corresponds to polarization rotation, and has a dispersive line shape of resonance. The quadrature component gives a measure of phase associated with the resonance, and shows a Lorentzian line shape either as a peak (positive phase) or a dip (negative phase). Both components show NMOR resonances with their centers corresponding non-zero B fields. The resonance at the center corresponds to the zero-field Hanle resonance discussed earlier. Frequency sidebands of modulated light give rise to higher-order NMOR resonances with zero-crossings (or centers) corresponding to $B = \pm n\,(\Omega_m/2\gamma) = \pm n(35.7\text{ mG})$ where $n = 1,3,5\ldots$.The Fourier series decomposition of a square wave modulation with 50% duty cycle suggests that the even-order frequency sidebands in laser excitation are absent. As a result, magnetic resonances corresponding to $n = 2,4, \ldots$ are not observed in the NMOR spectrum. Figure 5b shows the NMOR spectra using the in-phase component, by lowering the duty cycle of light modulation from 50% to 30%. For duty cycles 40% and 30%, second-order NMOR resonances corresponding to zero-crossings at $B = \pm n\,(\Omega_m/2\gamma) = \pm 71.4$ mG) are observed. The amplitude of second-order NMOR resonance is small compared to the first-order resonance due to reduced optical power in the second-order sideband of light. Nevertheless, the center of second-order NMOR resonance corresponds to higher B field, and therefore, it can be used in magnetometry to measure higher field.

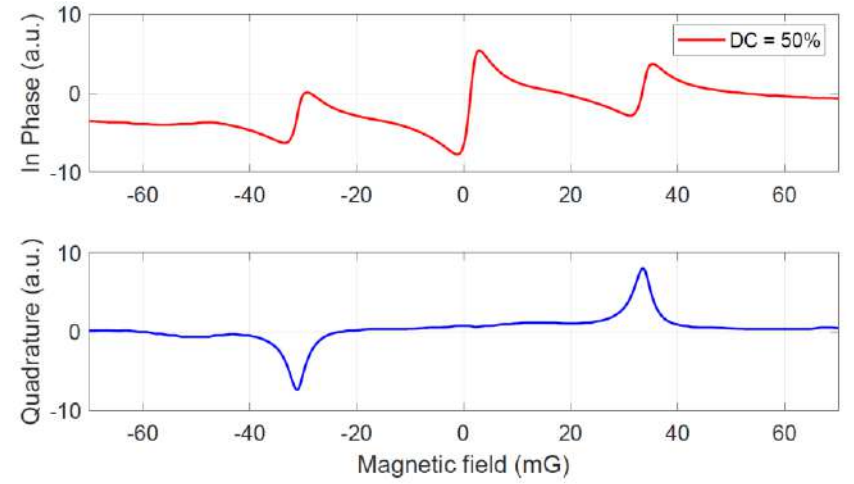

(a)

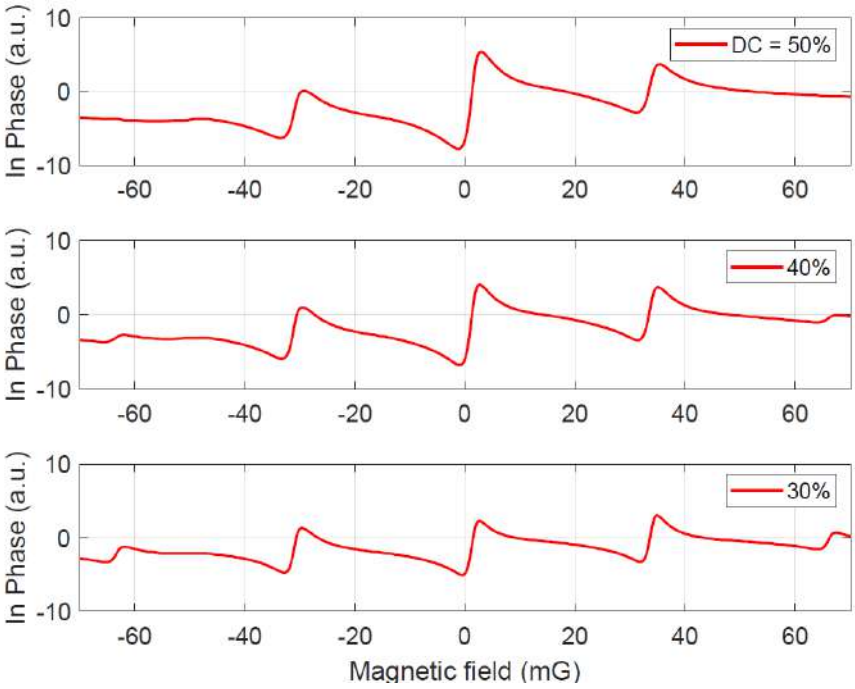

(b)

Fig 5. NMOR magnetic resonances measured using a two-channel lock-in-amplifier (a) in-phase and quadrature components obtained using pulsed modulation with Ω_m = 50 kHz and DC = 50%, (b) in-phase components obtained by lowering the duty cycle of modulation from 50% to 30%.

Due to frequency dependent phase referencing, lock-in-amplifier can be disadvantageous in measuring magnetic resonances for unknown field, as it may require changing the light modulation frequency Ω_m over a wide range. Alternatively, we have demonstrated a real-time correlation technique for measuring magnetic resonances without using lock-in-amplifer [15]. In this case, correlation is performed directly

between intensities I_H and I_V of the horizontal (H) and vertical (V) polarization channels after the polarizing beam splitter shown in Fig 3. Instead of subtracting the photodiode outputs, real-time correlation between photodiode outputs is performed using a high bandwidth digitizer board interfaced with LabView. We calculated the zero-delay intensity correlation $g^{(2)}(0)$ using the following definition:

$$g^2(0) = \frac{\langle \delta I_H(t)\ \delta I_V(t)\rangle}{\sqrt{\langle [\delta I_H(t)]^2\rangle\ \langle [\delta I_V(t)]^2\rangle}} \tag{1}$$

where δI_H and δI_V correspond to intensity fluctuations of H and V polarization components,

$$\langle \delta I_H(t)\rangle = \frac{1}{T}\int_t^{t+T} \delta I_H(t)dt$$

is the time averaged intensity and T corresponds to signal averaging time which in our experiment is set to 1 μs. The output signals from photodiodes are ac-coupled to measure intensity fluctuations δI_H and δI_V. These outputs are sampled by the digitizer board, and $g^{(2)}(0)$ is obtained by calculating Eq (1) in LabView. Magnetic resonances are measured by calculating the zero-delay correlation $g^{(2)}(0)$ in real-time while scanning the magnetic field (or modulation frequency). Intensity correlation $g^{(2)}(0)$ between two polarization channels can be interpreted as a correlation due to conversion of laser phase noise to amplitude noise by resonant interaction of laser with the atomic medium.

Figure 6a shows magnetic resonances measured in intensity correlation by sweeping the magnetic field (or Larmor frequency, Ω_L). We used laser excitation of $F_g = 2 \rightarrow F_e = 1$ transition in ^{87}Rb atoms, 40% duty cycle and 50 μW average power in modulated light (Ω_m 15 kHz). Correlation measurements are shown in the Fig 6 as discrete data points, and the solid blue line shows fitting of correlation measurements with Lorentzian functions. Higher harmonic resonances are observed as correlation peaks with their centers corresponding to $\Omega_L = \pm n\ (\Omega_m/2)$, n =1,2,…. Unlike lock-in detection, no correlation is observed near $\Omega_L = 0$. The amplitude of second-order resonance in correlation is found to be higher than the first-order. The widths of correlation peaks are not broadened by increasing the average power in laser excitation. In fact, at higher average power (> 200 μW), amplitudes of correlation peaks are substantially reduced due to population transfer from $F_g = 2$ to $F_g = 1$. Figure 6b shows magnetic resonances in correlation measurements obtained by sweeping the modulation frequency, Ω_m over a wide range of frequency from 10 to 210 kHz, while keeping the B (or Ω_L) fixed. The wide sweep allows us to observe the magnetic resonance with center at $\Omega_m = 2\ \Omega_L$ and its sub-harmonics with centers corresponding to $\Omega_m = 2\ \Omega_L/\ n$; n = 2,3… . Multiple noise peaks are also observed near the third sub-harmonic. The result shows that real-time correlation can be performed over a wide frequency range, thus making correlation technique viable for measuring unknown B field in magnetometry.

Next, we discuss magnetic resonances measured in fluorescence from laser excitation of D_2 transition in a sodium cell. The sodium cell used in our experiment also contains 10 Torr Ne buffer gas to prevent broadening due to transit-time effect on magnetic resonance. Fluorescence from sodium cell at 90º angle to the light propagation direction is detected using a light-sensitive avalanche photodiode (APD). In this experiment, magnetic field (or Ω_L) along $\hat{x}$-direction, perpendicular to light propagation direction ($\hat{z}$) is scanned. The laser beam is circularly polarized and modulated at fixed $\Omega_m = 20$ kHz with an average intensity of 0.25 mW/cm^2. Figure 7 shows magnetic resonances observed in fluorescence corresponding to two different duty cycles of light modulation. Maximum amplitudes of magnetic resonances are observed by locking the laser closer to the cross-over peak located midway between D_{2a} and D_{2b} transitions. The in-phase and quadrature signals are obtained from the lock-in amplifier by demodulating the fluorescence signal from the APD output at Ω_m. When the laser is modulated with 50% duty cycle (Fig 7a (first column)), two-photon resonance condition leads to magnetic resonances with centers at $\Omega_L = \pm\ \Omega_m$, as seen in both in-phase and quadrature-phase signals. Dips in in-phase signal indicate resonances due to dark states as discussed before.

The FWHM of magnetic resonance near zero magnetic field is measured approximately to be 3.2 mG (2.24 kHz). For duty cycle of 20% (Fig 7b (second column)), the in-phase signal shows resonances up to the third harmonic, and the quadrature signal shows resonances up to fourth harmonic. The quadrature signal is sensitive to the signal phase, and it can allow detection of very weak signals at high magnetic fields. Higher order resonances at lower duty cycles are formed due to the presence of Fourier components at integer multiples of at Ω_m in the modulated laser excitation. These results are being used as benchmark for our upcoming remote magnetometry experiments to be conducted with mesospheric sodium atoms.

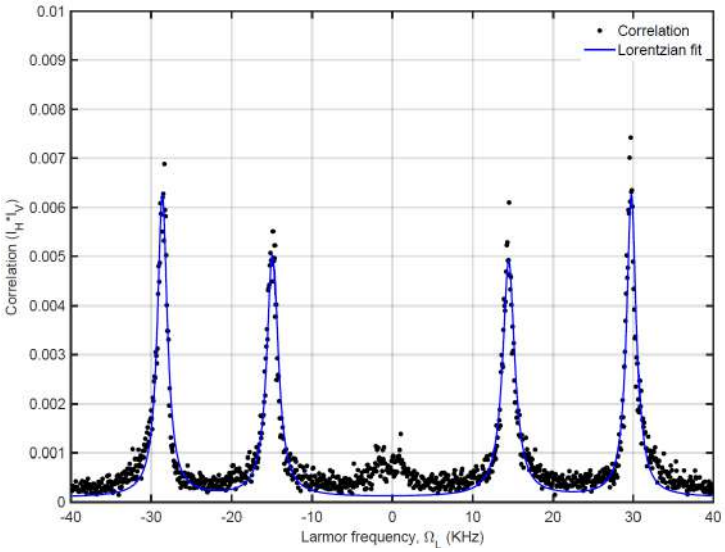

(a)

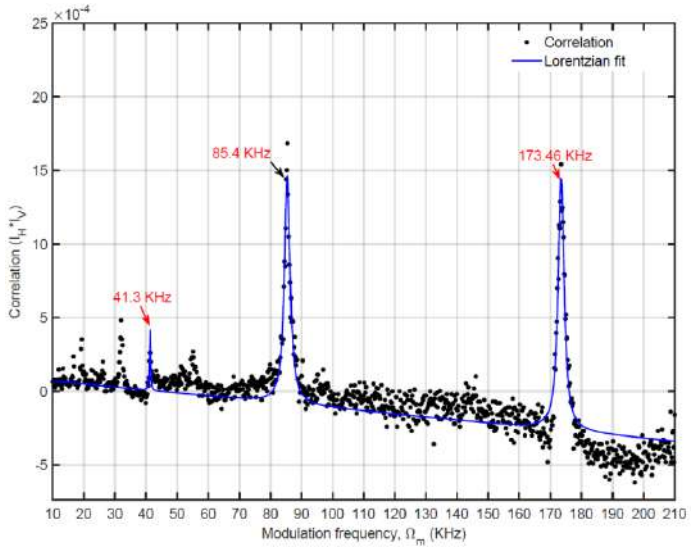

(b)

Fig 6. Magnetic resonances measured in intensity correlation $g^{(2)}(0)$ between H and V polarization components: (a) sweeping the Larmor frequency, Ω_L and (b) sweeping the modulation frequency Ω_m over a wide range from 10 to 210 kHz.

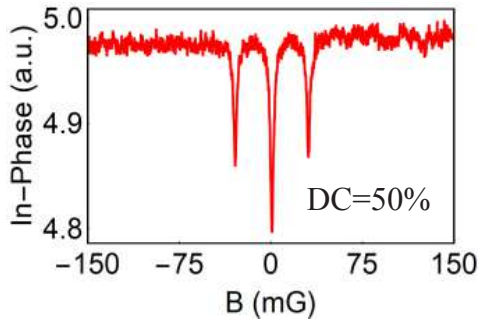

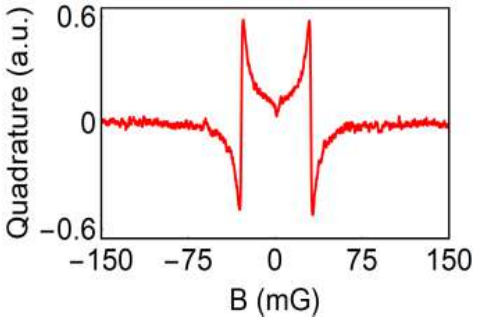

(a)

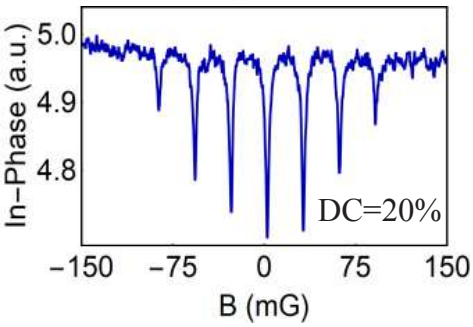

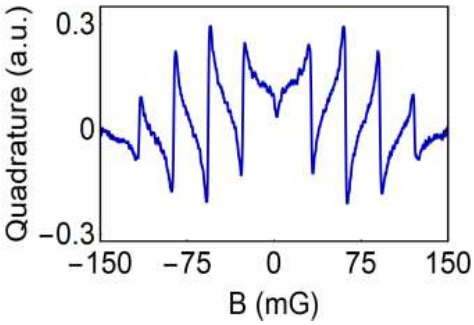

(b)

Fig 7. Magnetic resonances measured in fluorescence from a sodium cell: in-phase and quadrature signals corresponding to (a) 50% duty cycle, and (b) 20% duty cycle, at Ω_m = 20kHz.

5 Conclusions

In conclusion, we have investigated magnetic resonances produced by modulated laser beam excitation in the atomic medium. In particular, we studied NMOR resonances using laser excitation of D_1 transition in a rubidium cell containing pure isotope ^{87}Rb atoms, and also studied fluorescence resonance using laser excitation of D_2 transition in a sodium cell. The origin of these resonances are explained using Λ- systems and 'dark states' formed by multiple frequency components of the modulated laser beam. We used a theoretical model to simulate NMOR resonances produced in rubidium atoms for laser excitation with modulated light. We also demonstrated a new real-time correlation technique for measuring magnetic resonance with a wide modulation frequency scan. Present studies have improved our understanding of magnetic resonances for magnetometry applications.

References

1. Budker D, Kimball D F J, Optical Magnetometry, (Cambridge University Press), 2013.
2. Sander T H, Preusser J, Mhaskar R, Kitching J, Trahms L, Knappe S, "Magnetoencephalography with a chip-scale atomic magnetometer," *Biomed Opt Express*, 3(2012) 27167-27172.
3. Schultz G, Mhaskar R, Prouty M, Schultz G, Mhaskar R, Prouty M, Miller J, "Integration of micro-fabricated atomic magnetometers on military systems," *Proc SPIE*, 9823(2016)982318; doi.org/10.1117/12.2224192.
4. Schwindt P D D, Knappe S, Shah V, Hollberg L, Kitching J, Liew L A, Moreland J, "Chip-scale atomic magnetometer," *Appl Phys Lett*, 85(2004) 6409-6411.
5. Kitching J, Chip-scale atomic devices, Appl Phys Rev, 5(2018)31302; doi.org/10.1063/1.5026238
6. Budker D, Romalis M, Optical magnetometry, *Nat Phys*, 3(2007)227-234.
7. Kominis I K, Kornack T W, Allred J C, Romalis M V, A subfemtotesla multichannel atomic magnetometer, *Nat Phys*, 422(2003)596-599.
8. Budker D, Kimball D F, Rochester S M, Yashchuk V V, Zolotorev M, Sensitive magnetometry based on nonlinear magneto-optical rotation, *Phys Rev A*, 62(2003)43403; doi. org/10.1103/PhysRevA.62.043403
9. Acosta V, Ledbetter M P, Rochester S M, Budker D, Kimball D F J, Hovde D C, Gawlik W, Pustelny S, Zachorowski J, Yashchuk V V, Nonlinear magneto-optical rotation with frequency-modulated light in the geophysical field range, *Phys Rev A – At Mol Opt Phys*, 73(2006)1-8.
10. Gawlik W, Krzemien L, Pustelny S, Sangla D, Zachorowski J, Graf M, Sushkov A O, Budker D, Nonlinear Magneto-Optical Rotation with Amplitude-Modulated Light, *Appl Phys Lett*, 88(2006)131108; doi.org/10.1063/1.2190457
11. Higbie J M, Rochester S M, Patton B, Holzlohner R, Calia D B, Budker D, Magnetometry with mesospheric sodium, *Proc Natl Acad Sci*, 108(2011)3522-3525.
12. Warren Z, Shahriar M S, Tripathi R, Pati G S, Experimental and theoretical comparison of different optical excitation schemes for a compact coherent population trapping Rb vapor clock, *Metrologia*, 54(2017)418-431.
13. Renzoni F, Maichen W, Windholz L, Arimondo E, Coherent population trapping with losses observed on the Hanle effect of the D 1 sodium line, *Phys Rev A*, 55(1997)3710-3718.
14. Renzoni F, Zimmermann C, Verkerk P, Arimondo E, Enhanced absorption Hanle effect on the $F_g = F \rightarrow F_e = F + 1$ closed transitions, *J Opt B:Quantum Semiclassical Opt*, 7(2001)S7-S14.
15. Felinto D, Cruz L S, de Oliveira E A, Florez H M, de Miranda M H G, Nussenzveig P, Martinelli M, Tabosa J W R, Physical interpretation for the correlation spectra of electromagnetically-induced-transparency resonances, *Opt Express*, 21(2013)485-491.

[Received: 30.11.2019; accepted: 10.12.2019]

Gour Pati

Dr. Gour Pati is Professor of Physics and Engineering in the Division of Physics, Engineering, Mathematics and Computer Science (PEMaCS) at Delaware State University (DSU), Dover, DE. He received his Ph.D. in Physics and M.Tech in Applied Optics from the Indian Institute of Technology (IIT), Delhi in 1999, and 1993 respectively. He has done postdoctoral research at University of Colorado, MIT and Northwestern University from 1999 to 2007. He has published over 70 research articles in peer-reviewed journals, and conference proceedings. His current research interest includes coherent light-matter interaction, atomic clock, magnetometer, atom-based quantum sensing, and low-light-level nonlinear optical phenomena. Dr Pati is a 2019 Senior member of International Society for Optics and Photonics (SPIE). He is serving in the program committee of SPIE Conference on 'Optical, Opto-Atomic, and Entanglement-Enhanced Precision Metrology II' at SPIE Photonics West 2020.

Renu Tripathi

Dr. Renu Tripathi is Professor of Physics and Engineering in the Division of Physics, Engineering, Mathematics and Computer Science (PEMaCS) at Delaware State University (DSU), Dover, DE. She received her Ph.D. in Physics andM. Tech in Applied Optics from the Indian Institute of Technology (IIT), Delhi in 1999, and 1994 respectively. Prior to joining DSU in 2008, she conducted postdoctoral research at University of California, Irvine, MIT and Northwestern University, and worked as a laser scientist/engineer at California Institute of Technology, CA. Her current research includes alkali vapor magnetometry, polarimetric imaging LADAR, optical coherence tomography, nonlinear and fluorescent properties of diamond nitrogen vacancy (NV) emitters, slow and fast light, coherent light-matter interaction, and its application in precision sensing and measurement. She has published more than 80 peer reviewed journal articles and conference proceedings. She is a recipient of *DSU Faculty Excellence Award* for Research and Creative Activities in July 2017. Dr Tripathi is a *Senior Member* of Optical Society of America (OSA) and a *Senior Life Member* of International Society of Optical Engineering (SPIE). She is currently serving as a member of the Conference Program Committee on 'Optical, Opto-Atomic, and Entanglement-Enhanced Precision Metrology II', SPIE Photonics West Conference 2020.